

Ensemble modeling of black Pomfret (*Parastromateus niger*) habitat in the Taiwan Strait based on oceanographic variables

Sandipan Mondal^{1,2}, Ming An Lee^{Corresp., 1, 2, 3}, Yu-Kai Chen⁴, Yi-Chen Wang^{1, 2}

¹ Environmental Biology & Fishery Science, National Taiwan Ocean University, Keelung, Taiwan

² Center of Excellence for Ocean Engineering, National Taiwan Ocean University, Keelung, Taiwan

³ Doctoral degree program in Ocean Resource and Environmental Changes, National Taiwan Ocean University, Keelung, Taiwan

⁴ Coastal and Offshore Resource Research Center, Fisheries Research Institute, Council of Agriculture, Kaohsiung, Taiwan

Corresponding Author: Ming An Lee

Email address: malee@mail.ntou.edu.tw

This study used data from Taiwan's Fisheries Agency, including fishing location, effort, captures, and time, to evaluate the geographic distribution of *Parastromateus niger* in the Taiwan Strait. Generalized linear models (GLMs) based on six oceanographic parameters outperformed other species distribution models. The locations with the greatest standardized catch-per-unit-effort (S.CPUE) of *P. niger* had a sea surface temperature (SST) of 26.5°C–29.5°C, sea surface chlorophyll (SSC) level of 0.3–0.44 mg/m⁻³, sea surface salinity (SSS) of 33.4–34.4 psu, mixed layer depth of 10–14 m, sea surface height of 0.57–0.77 m, and eddy kinetic energy (EKE) of 0.603–0.794 m²/s⁻². The statistical results indicate that the major factors influencing species distribution are SSS, SSC level, and EKE and that SST is only a minor factor. An ensemble habitat model was formed through the combination of four well-performing single-algorithm models with no discernible bias. The largest annual distribution of S.CPUE and nominal CPUE was located in the ranges of 117°E–119°E and 22°N–24°N.

1 Ensemble modeling of Black Pomfret (*Parastromateus niger*) 2 habitat in the Taiwan Strait based on oceanographic 3 variables

4
5 Sandipan Mondal^{1,2}, and Ming-An Lee^{1,2,3*}, Yu-Kai Chen⁴ and Yi-Chen Wang^{1,2}

6 ¹Department of Environmental Biology Fisheries Science, National Taiwan Ocean University

7 ²Center of Excellence for Ocean Engineering, National Taiwan Ocean University, Keelung 20224, Taiwan

8 ³Doctoral degree program in Ocean Resource and Environmental Changes, National Taiwan Ocean
9 University, No.2, Beining Rd., Zhongzheng Dist., Keelung City 20224, Taiwan.

10 ⁴Coastal and Offshore Resource Research Center, Fisheries Research Institute, Council of Agriculture,
11 Keelung City 20224, Taiwan

12

13 * **Correspondence:** malee@mail.ntou.edu.tw

14

15 Abstract

16 The location, effort, number of captures, and time of fishing were all used in this study to assess
17 the geographic distribution of *Parastromateus niger* in the Taiwan Strait. Other species distribution
18 models performed worse than generalized linear models (GLMs) based on six oceanographic
19 parameters. The sea surface temperature (SST) was between 26.5°C and 29.5°C, the sea surface
20 chlorophyll (SSC) level was between 0.3-0.44 mg/m³, the sea surface salinity (SSS) was between
21 33.4°C and 34.4°C, the mixed layer depth was between 10°C and 14°C, the sea surface height was
22 between 0.57°C and 0.77°C, and the eddy kinetic energy (EKE) was between 0.603°C According
23 to the statistical findings, SST is merely a small effect compared to SSS, SSC level, and EKE in
24 terms of impacting species distribution. By combining four effective single-algorithm models with
25 no obvious bias, an ensemble habitat model was created. The ranges of 117°E-119°E and 22°N-
26 24°N have the highest annual distributions of S.CPUE and nominal CPUE.

27

28 **Keywords:** boosted regression tree (BRT), classification and regression tree (CART), ensemble
29 model, generalized additive model (GAM), generalized linear model (GLM).

30

31 1. Introduction

32 Species distribution models (SDMs) are the most common method of examining species habitat
33 patterns through the use of oceanographic elements; they are also referred to as habitat models,
34 ecological niche models, bioclimatic envelopes, and resource selection functions (Zimmerman et
35 al., 2010, Robinson et al., 2011, Beale & Lennon, 2012, Li & Wang, 2013 and Tikhonov et al.,
36 2020). Habitat models use mathematical representations of the current species distribution to
37 predict the future distribution by using an algorithm. Historically, the arithmetic mean and
38 geometric mean models (Xue et al., 2017; Li et al., 2016) based on the habitat appropriateness
39 index have been used. However, the adoption of various machine learning models has been
40 accelerated by technical advancement. Machine learning (ML) is a topic of study focused on

41 comprehending and developing "learning" techniques, or techniques that use data to improve
42 performance on a certain set of tasks. It's thought of as a part of artificial intelligence. Without
43 being expressly taught to do so, machine learning algorithms create a model using sample data,
44 also referred to as training data, in order to make predictions or judgments. Machine learning
45 algorithms are utilized in a broad variety of applications, such as in medical, email filtering, speech
46 recognition, agriculture, and computer vision, where it is difficult or unfeasible to design
47 traditional algorithms to do the desired tasks. Computational statistics, which focuses on making
48 predictions with computers, is closely related to a subset of machine learning, but not all machine
49 learning is statistical learning. The field of machine learning benefits from the tools, theory, and
50 application domains that come from the study of mathematical optimization. Data mining is a
51 related area of study that focuses on unsupervised learning for exploratory data analysis. Some
52 machine learning applications employ data and neural networks in a manner that resembles how a
53 biological brain functions. Machine learning is also known as predictive analytics when it comes
54 to solving business problems. Different advanced models like regression models, including
55 generalized linear models (GLMs) and generalized additive models (GAMs) as well as artificial
56 intelligence models such as gradient boosting models (Hosain et al., 2020), artificial neural
57 networks (Ahmad, 2019), classification and regression tree (CART) models (Youssef et al.,
58 2016)], and random forest models (Reisinger et al., 2018) are in use present days. Ensemble models
59 (Reisinger et al., 2021; Tabor & Koch 2021), which incorporate the forecasts of two or more
60 habitat models (ensemble members), exhibit superior performance and robustness compared with
61 single-algorithm models. The ensemble members may be identical or dissimilar habitat model
62 types, and each can be trained with the same or different training sets (Georgian et al., 2019).
63 Statistics like the mode or mean can be used to combine the ensemble members' predictions, and
64 sophisticated techniques are employed to determine the trustworthiness of each ensemble member
65 and the circumstances under which it can be relied upon (Abrhams et al., 2019). Many studies
66 released in the 1990s have shown the extensive use of ensemble learning techniques such core
67 bagging, boosting, and stacking. When a single model is insufficient, ensemble models can be used
68 for prediction. Considering bias in the model helps lower the predictive error variance. The current
69 study concentrated on ensemble modeling for the habitat of the black pomfret.

70 Black pomfret, or *Parastromateus niger* (Bloch, 1795), are small pelagic fish that live in the
71 inshore waters of the Indian Ocean and western Pacific Ocean off the coasts of East Africa,
72 southern Japan, and Australia (Liu, 2008). Black pomfret are found across the East China Sea and
73 South China Sea, are prevalent in the Taiwan Strait, and play a significant role in lighting purse
74 seine fisheries in Taiwan and in Fujian and Guangdong Provinces (Lu & Yan, 1985; Lu et al.,
75 1991). Black pomfret production is vital to the coastal fisheries of Taiwan. However, the *P. niger*
76 stock status in the Taiwan Strait (TS) recently collapsed (Ju et al., 2020), as evidenced by a
77 significant drop in the annual capture in Taiwanese waters between 2002 and 2019 (Taiwan
78 Fisheries Agency, 2019). Possible reasons behind this substantial decline in yield might be due to
79 a combination of high demand, unregulated fishing methods, climate change, and the overfishing
80 of *P. niger* (eg: Tao et al. 2012, Ju et al. 2020), aimed/mentioned by the United Nations Sustainable

81 Development Goal (SDG) 14 (Ntona & Morgera, 2018). To achieve SDG 14, overfishing must be
82 controlled which is related to the unsustainable fish stock whereas underexploited or partially
83 exploited levels are viable, the target of sustainable exploration.
84 Understanding *P.niger* habitat preferences and zones in-depth is essential for maintaining a species
85 stock that is ecologically acceptable. In order to assist keep the species stock within an ecologically
86 acceptable range, we thus used habitat modeling to evaluate the effects of the maritime
87 environment on the *P.niger* habitat (Figure 1). (SDG 14.4). To stop overfishing of *P.niger*, a
88 thorough study of its biological preferences and habitat regions may be helpful (SDG 14.6).

89

90 **Figure 1.** Study flowchart.

91

92 **2. Materials and Methods**

93 **2.1 Data Collection**

94 2.1.1. Fisheries Data

95 We collected information from Taiwanese fishing vessels (mostly coastal sea fishing, with gross
96 register tonnage ranging from 0 to less than 250 tons) about *P. niger* fisheries from January 2014
97 to December 2019 from Taiwan's Fisheries Agency. The spatial coverage of the monthly fisheries
98 data was 21°N–26°N and 116°E–123°E, with a resolution of 0.1°. The data provider did not specify
99 whether the reported weights were dry or wet. Various fishing gear was used, and gears data with
100 maximum catch contribution were only used in this study. The collected data included the year,
101 month, latitude and longitude, catch in kilograms, effort in hours, total catch weight in one location,
102 type of fishing gear used, and vessel identification number. Data on fishing depth and gear-soaking
103 time were unavailable.

104

105 2.1.2. Oceanographic Data

106 Seven oceanographic characteristics (Table 1) were gathered from several sources for the current
107 study: sea surface temperature (SST), sea surface salinity (SSS), mixed layer depth (MLD), sea
108 surface chlorophyll (SSC) level, sea surface height (SSH), meridional velocity (U), and zonal
109 velocity (V; Table 1). we calculated eddy kinetic energy (EKE) from U and V as follows: $EKE =$
110 $0.5(U^2 + V^2)$. The CMEMS eddy-resolving global ocean reanalysis product GLORYS12V1 (1/12°
111 horizontal resolution with 50 vertical levels;

112 <https://resources.marine.copernicus.eu/product->

113 [detail/GLOBAL_MULTIYEAR_PHY_001_030/INFORMATION](https://resources.marine.copernicus.eu/product-detail/GLOBAL_MULTIYEAR_PHY_001_030/INFORMATION))

114 was used to collect SST, SSS, MLD, SSH, U, and V data. Its processing level and coordinate
115 reference system are L4 and W, respectively. In addition, we gathered SSC data using the CMEMS
116 global ocean biogeochemical hindcast product FREEGLORYS2V4 (0.25° horizontal resolution,
117 75 vertical levels, daily temporal resolution;

118 <https://resources.marine.copernicus.eu/product->

119 [detail/GLOBAL_MULTIYEAR_BGC_001_029/INFORMATION](https://resources.marine.copernicus.eu/product-detail/GLOBAL_MULTIYEAR_BGC_001_029/INFORMATION)),

120 whose processing level and coordinate reference system are Level 4 and ETRS89 (EU-
121 recommended frame of reference for geodata for Europe 1), respectively.

122 These data were originally gathered between January 2014 and December 2019 and covered the
 123 geographic range of 116°E–123°E and 21°N–26°N. These data were interpolated using
 124 MATBLAB (version 2019a) to a 0.1° spatial resolution to match the fisheries data. The SSC data
 125 were interpolated to a monthly temporal resolution using MATLAB in addition to the
 126 oceanographic and fisheries data.

127

128 **Table 1.** Surface oceanographic data and their descriptions.

129

130 **2.2. Fisheries Data Standardization**

131 The relative abundance of *P. niger* was as assessed as the N.CPUE from a total of 55,852
 132 observations as follows (Dunn et al., 2000; Laurdisen et al., 2008):

133

134 $N.CPUE = (\text{catch in kilograms})/(\text{fishing effort in hours})$

135

136 The use of the popular GLM standardization technique and resulting bias-filtered N.CPUE data
 137 (Hazin et al., 2007; Hinton & Maunder, 2004; Tian et al., 2009) helped to lessen the effects of
 138 spatial data, including latitude (lat) and longitude (long); temporal data (year and month); and
 139 interaction factors (i.e., year*lat, lat*long, and year*long; Mondal et al., 2022; Mondal et al., 2021;
 140 Vayghan et al., 2020; Forrestal, 2019; Shono, 2004). The key benefits of employing a GLM for
 141 standardization include the exponential distribution of response variables and the ability to employ
 142 categorical predictors. A stepwise GLM was created using the stats package in RStudio (version
 143 3.6.0) using the aforementioned seven components (year, month, lat, long, year*lat, lat*long, and
 144 year*long). The family and procedure employed for GLM optimization were the Gaussian family
 145 and glm.fit, respectively. The GLM constructed for standardization was as follows:

146

147 $GLM: \log(N.CPUE) = \text{year} + \text{month} + \text{lat} + \text{long} + \text{interactions},$

148

149 where the interaction factors are year*lat, lat*long, and year*long.

150

151 **2.3. S.CPUE–Oceanographic Factor Relationship**

152 The correlations between the S.CPUE benchmark values and the aforementioned oceanographic
 153 factors were established to discern the preferred parameter ranges. We created suitability index
 154 (SI) curves for each oceanographic parameter using summed S with smoothing spline regression.
 155 The regression used S.CPUE as the dependent variable and all selected oceanographic elements as
 156 the explanatory variables. The SI curves were then normalized as follows using S.CPUE and the
 157 oceanographic variables:

158

159 $SI = (Y - Y_{\min})/(Y_{\max} - Y_{\min}),$

160

161 where Y_{\max} and Y_{\min} are respectively the maximum and minimum number of observations of
 162 S.CPUE or oceanographic factors; thus, SI has a range between 0 and 1, where Y is a simulated or

163 predicted value from Y_{max} to Y_{min} . An oceanographic factor range with a large SI value (>0.6)
164 (Mondal et al. 2021, Vayghan et al 2020, and Lee et al. 2021) suggested a favorable range for
165 S.CPUE.

166

167 **2.4. Single-Algorithm Habitat Model Development**

168 The current study incorporated four single-algorithm models, namely a GLM, GAM, boosted
169 regression tree (BRT) model, and CART model. Each modeling technique was optimized
170 according to the established protocol. We developed one model for each modeling technique in
171 RStudio and the six oceanographic factors (SST, SSS, MLD, SSH, SSC, and EKE), which were
172 regarded as predictor variables; S.CPUE was the response variable.

173 We used the Gaussian family and the generalized cross-validation of the *mgcv* package to construct
174 each GAM. We employed the Gaussian family and the *glm.fit* technique from the *stats* package to
175 create each GLM. Each BRT model was built using the Gini approach and the Gaussian family
176 from the *gbm* program; optimization included the use of 100 trees, seven interactions, and 0.65
177 bag fractions. The *rpart* package was used to build each CART model using the Gaussian family
178 and the CP technique. The CART models were optimized with a CP value of 0.1 and minimum
179 and maximum node counts of 1 and 6, respectively.

180

181 **2.5. Validation of Selected Single-Algorithm Habitat Models**

182 The fisheries data set ($n = 55,852$) was split into two portions using a random splitting technique
183 performed by the RStudio *caret* package at a ratio of 70 [$n(70) = 39,115$] to 30 [$n(30) = 16,737$] to
184 validate the single-algorithm models. For each single-algorithm model, three coefficients—
185 namely the Pearson correlation coefficient (R), root-mean-square error (RMSE), and mean
186 absolute error (MAE)—were computed for both portions of the data set. Little variation in the R,
187 RMSE, and MAE values for the two data sets was considered indicative of a well-performing
188 model with low bias.

189

190 **2.6. Ensemble Habitat Model Development**

191 We created an ensemble habitat model in the RStudio BIOMOD2 package (Georgian et al., 2019;
192 Alabia et al., 2016; Reisinger et al., 2021; Tarbor & Koch, 2021; Abrahms et al., 2019) to enhance
193 the power to predict the *P. niger* habitat. A weighted mean ensemble model of the *P. niger* habitat
194 was created after the performance of the single-algorithm models was assessed. If no discernible
195 bias was detected on the basis of the R, RMSE, and MAE values for the two data sets for a single-
196 algorithm model, the model was integrated into the ensemble model. Models exhibiting potential
197 bias were excluded.

198 After the creation of the ensemble habitat model, MATLAB was used to visualize the monthly
199 value predictions of the ensemble model along with the S.CPUE for each point in the study area.

200

201 **3. Results**

202

203 **3.1. Standardization of Fisheries Data**

204 Over 88% of the catches were captured by otter trawl nets, gill nets, and Taiwanese seines (Figure
205 2). Thus only these data were selected for the analysis. The full GLM (with all six factors) resulted
206 in an explained deviance and adjusted R^2 of 18.135% and 0.181, respectively. The residual
207 distribution and quantile–quantile (QQ) plots (Figure 3) of the full GLM exhibited no significant
208 fluctuation. Thus, the full GLM approach was used for the standardization of the *P. niger* fisheries
209 data.

210

211 **Figure 2.** Catches from fishing with different gear.

212 **Figure 3.** Residual distributions and QQ graphs for the final GLM with predictor variables.

213

214 **3.2. S.CPUE–Oceanographic Factor Relationships**

215 The SI curves created for the S.CPUE of *P. niger* against the six oceanographic factors are
216 illustrated in Figure 4. When the SI value exceeded 0.6, the ideal SST, SSC level, SSS, MLD,
217 SSH, and EKE ranges were 26.5°C–29.5°C, 0.3–0.44 mg/m³, 33.4–34.4 PSU, 10–14 m, 0.57–0.77
218 m, and 0.603–0.794 m²/s², respectively. The total standardized CPUE of *P. niger* reached its
219 maximum near the SST, SSC level, SSS, MLD, SSH, and EKE of 29.5°C, 0.36 mg/m³, 34.2 PSU,
220 12 m, 0.67 m, and 0.661–0.724 m²/s², respectively. These results indicate the preferred
221 oceanographic range of *P. niger* in the TS during the research period.

222

223 **Figure 4.** Environmental ranges of *P. niger* with SI values from 2014 to 2019.

224

225 **3.3. Contributions of Single Oceanographic Factors**

226 Table 2 presents the performance of different oceanographic factors in the single-algorithm
227 models. SSH was observed to be the most dominant oceanographic factor in all four single-
228 algorithm models. The second most crucial oceanographic factor was EKE, which ranked second
229 in all single-algorithm models except the GLM. SSC ranked third in all single-algorithm models
230 except the GLM. SST, which ranked last in all the models, was deemed the least critical parameter.
231 SSS was ranked fifth in all models but the GLM, in which it was the least influential.

232

233 **Table 2.** Predictive performance of six oceanographic factors in single-algorithm GAMs, GLMs,
234 BRT models, and CART models.

235

236 **3.4. Performance and Validation of Single-Algorithm Models**

237 Table 3 presents the predictive performance of the full (with all oceanographic factors) GAM,
238 GLM, BRT model, and CART model. The deviance explained by the full GAM, GLM, BRT
239 model, and CART model was 54.1%, 41.52%, 52.7%, and 49.5%, respectively. The correlation
240 values of the full GAM, GLM, BRT model, and CART model were 0.543, 0.415, 0.525, and 0.498,
241 respectively. Figure 5a, 5b, 5c, and 5d depict the performance of the selected GAM, GLM, BRT
242 model, and CART model, respectively.

243

244 **Table 3.** Predictive performance of full (all six oceanographic factors) GAM, GLM, BRT model,
245 and CART model.

246

247 **Figure 5.** Residual distributions and QQ plots for diagnostic analysis of the full (a) GAM and (b)
248 GLM, both with predictor variables. Full (c) BRT and (d) CART model performance along with
249 the decision trees of the final model.

250 Small differences in the coefficients (R, RMSE, and MAE) for the two randomly apportioned data
251 sets (70:30) indicated no significant bias in any predictive (Table 4) models, and the predictions
252 were mapped onto a 1° geographic grid.

253

254 **Table 4.** Validation of selected single-algorithm models through random splitting.

255

256 **3.5. Ensemble Habitat Prediction**

257 Because no discernible bias was detected on the basis of the R, RMSE, or MAE values for the 70%
258 and 30% portions of the data, the produced ensemble was selected for final prediction (Table 5).
259 Figure 6 presents the predicted CPUE (P.CPUE) and S.CPUE. A high annual S.CPUE was
260 distributed primarily in the ranges of 119°E–121°E and 21°N–25°N, the coastal waters of Taiwan.
261 Most S.CPUE values were >4 in these locations but <1 in the remaining study areas. P.CPUE
262 displayed a pattern indicating expansion to 26°N. Both S.CPUE and P.CPUE were between 0.1
263 and 5.

264

265 **Table 5.** Validation of ensemble model through random splitting.

266

267 **Figure 6.** P.CPUE from the ensemble habitat model, along with S.CPUE.

268

269 **4. Discussion**

270 The Kuroshio Current and coastal currents near Taiwan contribute to the diversity and productivity
271 of marine species. As a result, the prevalence of fleet-based fishing operations has grown
272 substantially throughout Taiwan's waters over the past 40 years. The fishing gear used in this
273 region includes purse seines, bottom and pelagic trawls, longlines, and gill and set nets (Fisheries
274 Agency, 1949–2019). However, the trend of overfishing beginning in the 1950s caused catches to
275 peak in 1980 and gradually decline afterward (Chen et al., 2018; Liao et al., 2019). Despite
276 frequent acknowledgment of the problematic state of coastal and offshore fisheries in Taiwanese
277 waters (Liu, 2013; Chen, 2006; Shao et al., 2011), few fish species have been studied. Notably,
278 the *P. niger* stocks in the waters close to Taiwan have drastically decreased (Ju et al., 2020).

279

280 **4.1 Spatial Distribution**

281 High annual S.CPUE values were observed primarily in the ranges of 119°E–121°E and 21°N–
282 26°N. The P.CPUE values displayed a comparable pattern, with extension to 26°N. This
283 distribution pattern may result from various factors.

284 First, the Kuroshio Current and coastal currents have boosted species diversity and productivity in
285 the waters near Taiwan (Naimullah et al., 2020a). The Kuroshio Branch Current (KBC), China

286 Coastal Current (CCC), and South China Sea (SCS) Current are three major currents that affect
287 the TS, which is located in the tropical to subtropical western Pacific. These currents influence the
288 fishing grounds and marine habitats of the East China Sea and SCS that border the TS to the north
289 and south, respectively (Naimullah et al., 2022). The KBC provides a favorable environment for
290 the diversified *P. niger* in the TS. The CCC offers a neritic water mass with low salinity and
291 temperature but high nutrient content because of its connection to the rivers of the Chinese
292 mainland (Shiah et al., 2000). Contrary to popular assumption, the KBC, which is derived from
293 the Kuroshio Current, has high salinity and temperature and a nutrient level comparable to that of
294 the CCC (Chung et al., 2001). These traits produce a water mass with physical characteristics
295 distinct from those of the surrounding water. Properties such as temperature and salinity affect the
296 distribution of *P. niger*.

297 Second, the KBC and CCC both contribute to upwelling. The bottom current in the TS flows
298 upward from the continental slope, and the surface current is primarily driven by wind (Naimullah
299 et al., 2020b). In addition, the eastern side of the TS receives occasional injections of water from
300 the Kuroshio Current. The aforementioned upwelling forces nutrient-rich, typically chilly water to
301 ascend to the surface. The nutrients “fertilize” the surface waters and thus support a high level of
302 biological production. Consequently, these fertilized TS zones may serve as ideal *P. niger* fishing
303 locations.

304 Third, the seafloor of the TS is intricate. The seabed topography and capes influence tidal currents,
305 which form counterclockwise eddies (Hsu et al., 2021). High chlorophyll concentrations outside
306 the estuary are transferred by these tidal currents to the ocean current and attract secondary
307 producers, including fish, crustaceans, and mollusks, and draw out *P. niger* for harvest.

308

309 **4.2 Habitat Modeling Approach for Sustainable Development**

310 The detailed information provided by habitat or spatial distribution modeling may assist in the
311 sustainable management of *P. niger*. The pervasive nature of the measurement error inherent to
312 models of species and habitat distribution may render such models unable to contribute to spatial
313 economic optimization for sustainable planning. However, SDMs can potentially serve as heuristic
314 tools for addressing oceanic environmental challenges. We emphasize the contextual application
315 of such models.

316 Identification of fishing grounds that are underutilized or only partially utilized can be made easier
317 using habitat models. The predicted accuracy of single-algorithm models, however, can
318 occasionally be impacted by data changes, leading to unduly optimistic or gloomy predictions. As
319 a result, the current work used an ensemble modeling strategy. We merged and trained several
320 single-algorithm models, often known as weak learners, to address the same issue. Weak learners
321 ultimately produce ensemble models that are more accurate because, despite completing tasks
322 poorly when working alone, they collaborate with other weak learners to become strong
323 learners. The easy identification of fishing grounds crucially enhances fisheries revenue and
324 reduces fishing effort, travel time, fuel consumption, and cost. However, the likelihood of such
325 simplified identification of fishing grounds to result in overfishing highlights the relevance of the

326 SDGs. The adoption of SDG 14 has sparked discussion about ocean health and its importance to
327 the future of the planet (Ntona & Morgera, 2018). In here the most important aspect is the
328 conservation. Conservation measures can be taken in the overexploited areas and SDM can be
329 used to identify initially the distribution zone of any particular species. Condition of these high or
330 low catch zone can be examined through stock assessment to over or underexploited areas. The
331 SDG targets are intended address the major problems threatening ocean resources, such as
332 overfishing and climate change, but doing so requires emphases on the socioeconomic dimensions
333 of ocean politics and the distinct positions of the least developed countries and small island states.
334 The SDGs have garnered institutional acceptance since their adoption (Friess et al., 2019;
335 Sturesson et al., 2018). Understanding the habitat of *P. niger* in the TS may facilitate the
336 sustainable management of the species. The primary aim of SDG 14.4 is biologically sustainable
337 fish stock levels. Habitat modeling can play a crucial role in achieving this goal by identifying the
338 *P. niger* habitat in the TS. Additionally, SDG 14.5 focuses on conservation in coastal and marine
339 areas. Highly exploited areas can be declared protected areas through temporary fishing
340 prohibition to promote stock sustainability. SDG 14.6 calls for an end to overfishing subsidies.
341 Subsidies for fishing vessels traveling to less-exploited areas should be discontinued to avoid
342 overfishing. The sustainability of the oceans and their resources can also be promoted through the
343 enhancement of scientific understanding, research, and the transfer of marine technology. Related
344 policies should consider the Criteria and Guidelines of the Intergovernmental Oceanographic
345 Commission (SDG 14.a), support small-scale fisheries (SDG 14.b), and implement and uphold
346 international maritime law (SDG 14.c). The modeling of species distribution or habitats may
347 constitute the initial stage in sustainability research (Figure 7).

348

349 **4.3 Importance of the Study**

350 Fisheries management organizations have developed and embraced ecosystem-based management
351 techniques in recent years, improving public awareness of the contribution of fisheries to the
352 provision of marine ecosystem services (Kenny et al., 2018). The vital ecosystem services
353 provided by ocean resources are fundamental to the future of the planet. Such services provide a
354 considerable source of wealth and revenue, and their significance will continue to grow with the
355 rising demand for land-based natural resources (Virto, 2018). However, the ability of oceans and
356 their resources to meet the needs of their species is threatened (Neumann et al., 2017). Scientists
357 lack a full understanding of the environmental impacts of overfishing, other destructive fishing
358 practices, and ocean warming, which has caused rising sea levels and the expansion of ocean
359 acidification and hypoxic or dead zones. Some of the greatest threats stem from the introduction
360 of invasive species, primarily due to human activity. As new, capital-intensive methods of resource
361 extraction gain popularity and less technologically advanced nations fall behind in the competition
362 for limited maritime resources, the seas could become an arena that exacerbates global inequality
363 (Griggs et al., 2017). As a result, many people may be forced to change or drastically reduce their
364 demands on ocean ecosystems. Furthermore, scientists anticipate that ocean warming and
365 escalating climate change will significantly influence the lives of millions worldwide.

366 The current study identified the detailed habitat preferences and zones of *P. niger* to further the
367 maintenance of ecologically acceptable levels of species stock (SDG 14.4). A proper
368 understanding of habitat preferences and zones can help to prevent the overfishing of *P. niger*
369 (SDG 14.6). We plan to conduct future research on the predicted effects of climate change on *P.*
370 *niger* through habitat-based modeling and to offer recommendations for sustainability.

371

372 **Figure 7.** Habitat modeling approach for sustainable development with SDG interactions.

373

374 5. Conclusion

375 This study used a variety of oceanographic characteristics to pinpoint the geographic range of *P.*
376 *niger* in the TS. Due to the GLM approach's superior performance to other models, we chose it for
377 standardization. Near the SST, SSC level, SSS, MLD, SSH, and EKE of 29.5°C, 0.36 mg/m³, 34.2
378 PSU, 12 m, 0.67 m, and 0.661-0.724 m²/s², respectively, the *P. niger* S.CPUE attained its highest
379 value. According to the statistical analysis of our ensemble model, SST is the least important
380 component and SSH and EKE are the key factors affecting the *P. niger* distribution. The largest
381 yearly *P.*CPUE distribution followed by the largest annual S.CPUE distribution were found in the
382 regions of 21°N-26°N and 119°E-121°E.

383

384 **Author Contributions:** Conceptualization, S.M. and M.A.L.; methodology, M.A.L. and S.M.;
385 software, S.M.; validation, M.A.L.; formal analysis, S.M.; investigation, M.A.L. and Y.C.W.;
386 resources, M.A.L. and Y.C.W.; writing (original draft preparation), S.M.; writing (review and
387 editing), M.A.L.; visualization, Y.C.W. All authors have read and approved of the published
388 version of the manuscript.

389

390 **Funding:** This research was financed by the Council of Agriculture (111AS-6.4.2-FA-F1) and the
391 National Science and Technology Council of Taiwan (NSTC110-2621-M-019-004).

392

393 **Acknowledgments:** We thank the anonymous reviewers and editors for their valuable comments
394 and suggestions, as well as the team members of the Taiwan Fisheries Agency and National
395 Science and Technology Council of Taiwan for their assistance in data preparation.

396

397 References

398 1. Tikhonov, G., Opedal, Ø.H., Abrego, N., Lehikoinen, A., de Jonge, M.M., Oksanen, J. and Ovaskainen, O.,
399 2020. Joint species distribution modelling with the R-package Hmsc. *Methods in ecology and evolution*,
400 11(3), pp.442-447.

401 2. Li, X. and Wang, Y., 2013. Applying various algorithms for species distribution modelling. *Integrative*
402 *zoology*, 8(2), pp.124-13.

403 3. Beale, C.M. and Lennon, J.J., 2012. Incorporating uncertainty in predictive species distribution modelling.
404 *Philosophical Transactions of the Royal Society B: Biological Sciences*, 367(1586), pp.247-258.

405 4. Robinson, L.M., Elith, J., Hobday, A.J., Pearson, R.G., Kendall, B.E., Possingham, H.P. and Richardson,
406 A.J., 2011. Pushing the limits in marine species distribution modelling: lessons from the land present
407 challenges and opportunities. *Global Ecology and Biogeography*, 20(6), pp.789-802.

- 408 5. Zimmermann, N.E., Edwards Jr, T.C., Graham, C.H., Pearman, P.B. and Svenning, J.C., 2010. New trends
409 in species distribution modelling. *Ecography*, 33(6), pp.985-989.
- 410 6. Xue, Y., Guan, L., Tanaka, K., Li, Z., Chen, Y. and Ren, Y., 2017. Evaluating effects of rescaling and
411 weighting data on habitat suitability modeling. *Fisheries Research*, 188, pp.84-94.
- 412 7. Li, G., Cao, J., Zou, X., Chen, X. and Runnebaum, J., 2016. Modeling habitat suitability index for Chilean
413 jack mackerel (*Trachurus murphyi*) in the South East Pacific. *Fisheries Research*, 178, pp.47-60.
- 414 8. Azzellino, A., Panigada, S., Lanfredi, C., Zanardelli, M., Airoidi, S. and di Sciara, G.N., 2012. Predictive
415 habitat models for managing marine areas: spatial and temporal distribution of marine mammals within the
416 Pelagos Sanctuary (Northwestern Mediterranean sea). *Ocean & coastal management*, 67, pp.63-74.
- 417 9. Zhang, T., Song, L., Yuan, H., Song, B. and Ebango Ngando, N., 2021. A comparative study on habitat
418 models for adult bigeye tuna in the Indian Ocean based on gridded tuna longline fishery data. *Fisheries
419 Oceanography*, 30(5), pp.584-607.
- 420 10. Hossain, M.S., Sarker, S., Sharifuzzaman, S.M. and Chowdhury, S.R., 2020. Primary productivity connects
421 hilsa fishery in the Bay of Bengal. *Scientific reports*, 10(1), pp.1-16.
- 422 11. Ahmad, H., 2019. Machine learning applications in oceanography. *Aquatic Research*, 2(3), pp.161-169.
- 423 12. Youssef, A.M., Pourghasemi, H.R., Pourtaghi, Z.S. and Al-Katheeri, M.M., 2016. Landslide susceptibility
424 mapping using random forest, boosted regression tree, classification and regression tree, and general linear
425 models and comparison of their performance at Wadi Tayyah Basin, Asir Region, Saudi Arabia. *Landslides*,
426 13(5), pp.839-856.
- 427 13. Reisinger, R.R., Raymond, B., Hindell, M.A., Bester, M.N., Crawford, R.J., Davies, D., de Bruyn, P.N.,
428 Dilley, B.J., Kirkman, S.P., Makhado, A.B. and Ryan, P.G., 2018. Habitat modelling of tracking data from
429 multiple marine predators identifies important areas in the Southern Indian Ocean. *Diversity and
430 Distributions*, 24(4), pp.535-550.
- 431 14. Reisinger, R.R., Friedlaender, A.S., Zerbini, A.N., Palacios, D.M., Andrews-Goff, V., Dalla Rosa, L.,
432 Double, M., Findlay, K., Garrigue, C., How, J. and Jenner, C., 2021. Combining regional habitat selection
433 models for large-scale prediction: Circumpolar habitat selection of Southern Ocean humpback whales.
434 *Remote Sensing*, 13(11), p.2074.
- 435 15. Tao, Y., Mingru, C., Jianguo, D., Zhenbin, L., and Shengyun, Y. (2012). Age and growth changes and
436 population dynamics of the black pomfret (*Parastromateus niger*) and the frigate tuna (*Auxis thazard thazard*),
437 in the Taiwan Strait. *Lat. Am. J. Aquat. Res.* 40, 649–656.
- 438 16. Tabor, J.A. and Koch, J.B., 2021. Ensemble models predict invasive bee habitat suitability will expand under
439 future climate scenarios in Hawai'i. *Insects*, 12(5), p.443.
- 440 17. Georgian, S.E., Anderson, O.F. and Rowden, A.A., 2019. Ensemble habitat suitability modeling of
441 vulnerable marine ecosystem indicator taxa to inform deep-sea fisheries management in the South Pacific
442 Ocean. *Fisheries research*, 211, pp.256-274.
- 443 18. Abrahms, B., Welch, H., Brodie, S., Jacox, M.G., Becker, E.A., Bograd, S.J., Irvine, L.M., Palacios, D.M.,
444 Mate, B.R. and Hazen, E.L., 2019. Dynamic ensemble models to predict distributions and anthropogenic risk
445 exposure for highly mobile species. *Diversity and Distributions*, 25(8), pp.1182-1193.
- 446 19. Reisinger, R.R., Raymond, B., Hindell, M.A., Bester, M.N., Crawford, R.J., Davies, D., de Bruyn, P.N.,
447 Dilley, B.J., Kirkman, S.P., Makhado, A.B. and Ryan, P.G., 2018. Habitat modelling of tracking data from
448 multiple marine predators identifies important areas in the Southern Indian Ocean. *Diversity and
449 Distributions*, 24(4), pp.535-550.
- 450 20. Rowden, A.A., Anderson, O.F., Georgian, S.E., Bowden, D.A., Clark, M.R., Pallentin, A. and Miller, A.,
451 2017. High-resolution habitat suitability models for the conservation and management of vulnerable marine
452 ecosystems on the Louisville Seamount Chain, South Pacific Ocean. *Frontiers in Marine Science*, 4, p.335.

- 453 21. Alabia, I.D., Saitoh, S.I., Igarashi, H., Ishikawa, Y., Usui, N., Kamachi, M., Awaji, T. and Seito, M., 2016.
454 Ensemble squid habitat model using three-dimensional ocean data. *ICES Journal of Marine Science*, 73(7),
455 pp.1863-1874.
- 456 22. Liu, R.Y. 2008. Checklist of marine biota of China Seas. Science Press, Beijing, 1267 pp.
- 457 23. Lu, Z. & Y. Youming. 1985. Age and growth of *Parastromateus niger* in Western Taiwan Strait. *J.*
458 *Fujian Fish.*, 3: 7-13.
- 459 24. Lu, Z., D. Quanshui & Y. Youming. 1991. Growth and mortality of *Auxis thazard* in the Taiwan
460 Strait and its adjacent sea. *J. Fish. China*, 15(3): 228-235.
- 461 25. Taiwan Fisheries Agency, 2019.
- 462 26. Ntona, M. and Morgera, E., 2018. Connecting SDG 14 with the other Sustainable Development Goals
463 through marine spatial planning. *Marine Policy*, 93, pp.214-222.
- 464 27. Cormier, R. and Elliott, M., 2017. SMART marine goals, targets and management—is SDG 14 operational or
465 aspirational, is ‘Life Below Water’ sinking or swimming? *Marine pollution bulletin*, 123(1-2), pp.28-33.
- 466 28. Mugagga, F. and Nabaasa, B.B., 2016. The centrality of water resources to the realization of Sustainable
467 Development Goals (SDG). A review of potentials and constraints on the African continent. *International*
468 *Soil and Water Conservation Research*, 4(3), pp.215-223.
- 469 29. Ju, P., Tian, Y., Chen, M., Yang, S., Liu, Y., Xing, Q. and Sun, P., 2020. Evaluating stock status of 16
470 commercial fish species in the coastal and offshore waters of Taiwan using the CMSY and BSM methods.
471 *Frontiers in Marine Science*, 7, p.618.
- 472 30. Dunn, A., Harley, S.J., Doonan, I.J. and Bull, B., 2000. Calculation and interpretation of catch-per-unit effort
473 (CPUE) indices. *New Zealand fisheries assessment report*, 1, p.44.
- 474 31. Lauridsen, T.L., Landkildehus, F., Jeppesen, E., Jørgensen, T.B. and Søndergaard, M., 2008. A comparison
475 of methods for calculating Catch Per Unit Effort (CPUE) of gill net catches in lakes. *Fisheries Research*,
476 93(1-2), pp.204-211.
- 477 32. Hazin, H.G., Hazin, F., Travassos, P., Carvalho, F.C. and Erzini, K., 2007. Standardization of swordfish
478 CPUE series caught by Brazilian longliners in the Atlantic Ocean, by GLM, using the targeting strategy
479 inferred by cluster analysis. *Collect. Vol. Sci. Pap. ICCAT*, 60(6), pp.2039-2047.
- 480 33. Hinton, M.G. and Maunder, M.N., 2004. Methods for standardizing CPUE and how to select among them.
481 *Col. Vol. Sci. Pap. ICCAT*, 56(1), pp.169-177.
- 482 34. Tian, S., Chen, X., Chen, Y., Xu, L. and Dai, X., 2009. Standardizing CPUE of *Ommastrephes bartramii* for
483 Chinese squid-jigging fishery in Northwest Pacific Ocean. *Chinese Journal of Oceanology and Limnology*,
484 27(4), pp.729-739.
- 485 35. Mondal, S., Vayghan, A.H., Lee, M.A., Wang, Y.C. and Semedi, B., 2021. Habitat suitability modeling for
486 the feeding ground of immature albacore in the southern Indian Ocean using satellite-derived sea surface
487 temperature and chlorophyll data. *Remote Sensing*, 13(14), p.2669.
- 488 36. Vayghan, A.H., Lee, M.A., Weng, J.S., Mondal, S., Lin, C.T. and Wang, Y.C., 2020. Multisatellite-based
489 feeding habitat suitability modeling of albacore tuna in the southern Atlantic ocean. *Remote Sensing*, 12(16),
490 p.2515.
- 491 37. Mondal, S., Wang, Y.C., Lee, M.A., Weng, J.S. and Mondal, B.K., 2022. Ensemble Three-Dimensional
492 Habitat Modeling of Indian Ocean Immature Albacore Tuna (*Thunnus alalunga*) Using Remote Sensing
493 Data. *Remote Sensing*, 14(20), p.5278..
- 494 38. Forrestal, F.C., Schirripa, M., Goodyear, C.P., Arrizabalaga, H., Babcock, E.A., Coelho, R., Ingram, W.,
495 Laretta, M., Ortiz, M., Sharma, R. and Walter, J., 2019. Testing robustness of CPUE standardization and
496 inclusion of environmental variables with simulated longline catch datasets. *Fisheries research*, 210, pp.1-

- 497 13.
- 498 39. Shono, H., 2004. A review of some statistical approaches used for CPUE standardization. *Bulletin of the*
499 *Japanese Society of Fisheries Oceanography (Japan)*.
- 500 40. Georgian, S.E., Anderson, O.F. and Rowden, A.A., 2019. Ensemble habitat suitability modeling of
501 vulnerable marine ecosystem indicator taxa to inform deep-sea fisheries management in the South Pacific
502 Ocean. *Fisheries research*, 211, pp.256-274.
- 503 41. Alabia, I.D., Saitoh, S.I., Igarashi, H., Ishikawa, Y., Usui, N., Kamachi, M., Awaji, T. and Seito, M., 2016.
504 Ensemble squid habitat model using three-dimensional ocean data. *ICES Journal of Marine Science*, 73(7),
505 pp.1863-1874.
- 506 42. Reisinger, R.R., Friedlaender, A.S., Zerbini, A.N., Palacios, D.M., Andrews-Goff, V., Dalla Rosa, L.,
507 Double, M., Findlay, K., Garrigue, C., How, J. and Jenner, C., 2021. Combining regional habitat selection
508 models for large-scale prediction: Circumpolar habitat selection of Southern Ocean humpback whales.
509 *Remote Sensing*, 13(11), p.2074.
- 510 43. Tabor, J.A. and Koch, J.B., 2021. Ensemble models predict invasive bee habitat suitability will expand under
511 future climate scenarios in Hawai'i. *Insects*, 12(5), p.443.
- 512 44. Abrahms, B., Welch, H., Brodie, S., Jacox, M.G., Becker, E.A., Bograd, S.J., Irvine, L.M., Palacios, D.M.,
513 Mate, B.R. and Hazen, E.L., 2019. Dynamic ensemble models to predict distributions and anthropogenic risk
514 exposure for highly mobile species. *Diversity and Distributions*, 25(8), pp.1182-1193.
- 515 45. Chen, J.L., Lin, Y.S. and Chuang, C.T., 2018. Improving the management of Taiwanese fishery resource
516 conservation zones based on public perceptions and willingness to pay for ecosystem services. *Journal of*
517 *Coastal Conservation*, 22(2), pp.385-398.
- 518 46. Liao, C.P., Huang, H.W. and Lu, H.J., 2019. Fishermen's perceptions of coastal fisheries management
519 regulations: Key factors to rebuilding coastal fishery resources in Taiwan. *Ocean & Coastal Management*,
520 172, pp.1-13.
- 521 47. Liu, W.H., 2013. Managing the offshore and coastal fisheries in Taiwan to achieve sustainable development
522 using policy indicators. *Marine Policy*, 39, pp.162-171.
- 523 48. Chen, J.L., 2006. A study on the planning and management of fishery resource conservation areas in Taiwan.
524 National Taiwan Ocean University, Keelung (in Chinese).
- 525 49. Shao, K.T., Soong, K.Y., Lin, C.W., Wu, S.P., Chan, T.Y. and Chang, J.S., 2011. Investigation and planning
526 of fishery resources conservation zones and rare species. Fishery Agency, Taipei (in Chinese).
- 527 50. Kenny, A.J., Campbell, N., Koen-Alonso, M., Pepin, P. and Diz, D., 2018. Delivering sustainable fisheries
528 through adoption of a risk-based framework as part of an ecosystem approach to fisheries management.
529 *Marine Policy*, 93, pp.232-240.
- 530 51. Ntona, M. and Morgera, E., 2018. Connecting SDG 14 with the other Sustainable Development Goals
531 through marine spatial planning. *Marine Policy*, 93, pp.214-222.
- 532 52. Friess, D.A., Aung, T.T., Huxham, M., Lovelock, C., Mukherjee, N. and Sasmito, S., 2019. SDG 14: life
533 below water—impacts on mangroves. *Sustainable Development Goals*, 445, pp.445-481.
- 534 53. Stuesson, A., Weitz, N. and Persson, Å., 2018. SDG 14: Life Below Water. A Review of Research Needs.
535 Technical annex to the Formas report ForskningfÅr Agenda, 2030.
- 536 54. Virto, L.R., 2018. A preliminary assessment of the indicators for Sustainable Development Goal (SDG) 14
537 "Conserve and sustainably use the oceans, seas and marine resources for sustainable development". *Marine*
538 *Policy*, 98, pp.47-57.
- 539 55. Neumann, B., Ott, K. and Kenchington, R., 2017. Strong sustainability in coastal areas: a conceptual
540 interpretation of SDG 14. *Sustainability science*, 12(6), pp.1019-1035.

- 541 56. Griggs, D.J., Nilsson, M., Stevance, A. and McCollum, D., 2017. A guide to SDG interactions: from science
542 to implementation. International Council for Science, Paris.
- 543 57. Naimullah, M., Lan, K.W., Liao, C.H., Hsiao, P.Y., Liang, Y.R. and Chiu, T.C., 2020. Association of
544 environmental factors in the taiwan strait with distributions and habitat characteristics of three swimming
545 crabs. *Remote Sensing*, 12(14), p.2231.
- 546 58. Naimullah, M., Lee, W.Y., Wu, Y.L., Chen, Y.K., Huang, Y.C., Liao, C.H. and Lan, K.W., 2022. Effect of
547 soaking time on targets and bycatch species catch rates in fish and crab trap fishery in the southern East China
548 Sea. *Fisheries Research*, 250, p.106258.
- 549 59. Shiah, F.K., Chung, S.W., Kao, S.J., Gong, G.C. and Liu, K.K., 2000. Biological and hydrographical
550 responses to tropical cyclones (typhoons) in the continental shelf of the Taiwan Strait. *Continental Shelf
551 Research*, 20(15), pp.2029-2044.
- 552 60. Chung, S.W., Jan, S. and Liu, K.K., 2001. Nutrient fluxes through the Taiwan Strait in spring and summer
553 1999. *Journal of Oceanography*, 57(1), pp.47-53.
- 554 61. Naimullah, M., Lan, K.W., Liang, Y.R., Hsiao, P.Y., Chiu, T.C. and Liao, C.H., 2020. Distribution and
555 habitat characteristics of three important commercial swimming crab (Crustacea: Decapoda: Portunidae)
556 related with the environmental factors in Taiwan Strait.

Table 1 (on next page)

Surface oceanographic data sources and their descriptions

1 **Table 1.** Surface oceanographic data sources and their descriptions.

Environmental data	Abbreviation	Unit	Spatial resolution	Temporal resolution
Sea surface temperature	SST	°C	0.083° × 0.083°	Monthly
Sea surface salinity	SSS	psu		
Mixed layer depth	MLD	m		
Sea surface height above geoid	SSH			
Meridional velocity	U	ms ⁻¹		
Zonal velocity	V			
Sea surface chlorophyll	SSC	mgm ⁻³	0.25° × 0.25°	Daily

2

Table 2 (on next page)

The performance of different oceanographic factors in approaches based on GAMs, GLMs, BRTs, and CARTs

- 1 **Table 2.** The performance of different oceanographic factors in approaches based on GAMs,
- 2 GLMs, BRTs, and CARTs.

Single-Algorithm	SST		SSC		SSS		MLD		SSH		EKE	
	<i>Dev.</i>	<i>Rank</i>										
GAM	7.68	6	19.4	3	13.7	5	13.8	4	33.5	1	21.6	2
GLM	1.41	5	12.27	2	0.01	6	11.76	3	31.34	1	10.74	4
BRT	9.3	6	20.9	3	14.1	5	16.1	4	34.6	1	22.1	2
RF	8.9	6	18.5	3	10.9	5	15.1	4	33.2	1	20.6	2

3

Table 3 (on next page)

The predictive performance of full models (with all oceanographic factors) of GAM, GLM, BRT, and CART

- 1 **Table 3.** The predictive performance of full models (with all oceanographic factors) of GAM,
- 2 GLM, BRT, and CART.

Single-Algorithm	R²	Dev. Exp. (%)
GAM	0.543	54.1
GLM	0.415	41.52
BRT	0.525	52.7
CART	0.498	49.5

3

Table 4 (on next page)

Validation of selected single-algorithm models through random splitting

1 **Table 4.** Validation of selected single-algorithm models through random splitting.

Single algorithm	70% (<i>n</i> = 39,115)			30% (<i>n</i> = 16,737)		
	R ²	RMSE	MAE	R ²	RMSE	MAE
GAM	0.479	1.452	1.344	0.482	1.448	1.343
GLM	0.361	1.454	1.331	0.345	1.455	1.332
BRT	0.528	0.503	0.373	0.527	0.502	0.371
CART	0.496	0.516	0.387	0.521	0.504	0.372

2

Table 5 (on next page)

Ensemble habitat model's validation through random splitting

1 **Table 5.** Ensemble habitat model's validation through random splitting.

<i>70% (n = 39,115)</i>			<i>30% (n = 16,737)</i>		
R²	RMSE	MAE	R²	RMSE	MAE
0.624	1.311	1.475	0.621	1.333	1.483

2

Figure 1

Study flowchart

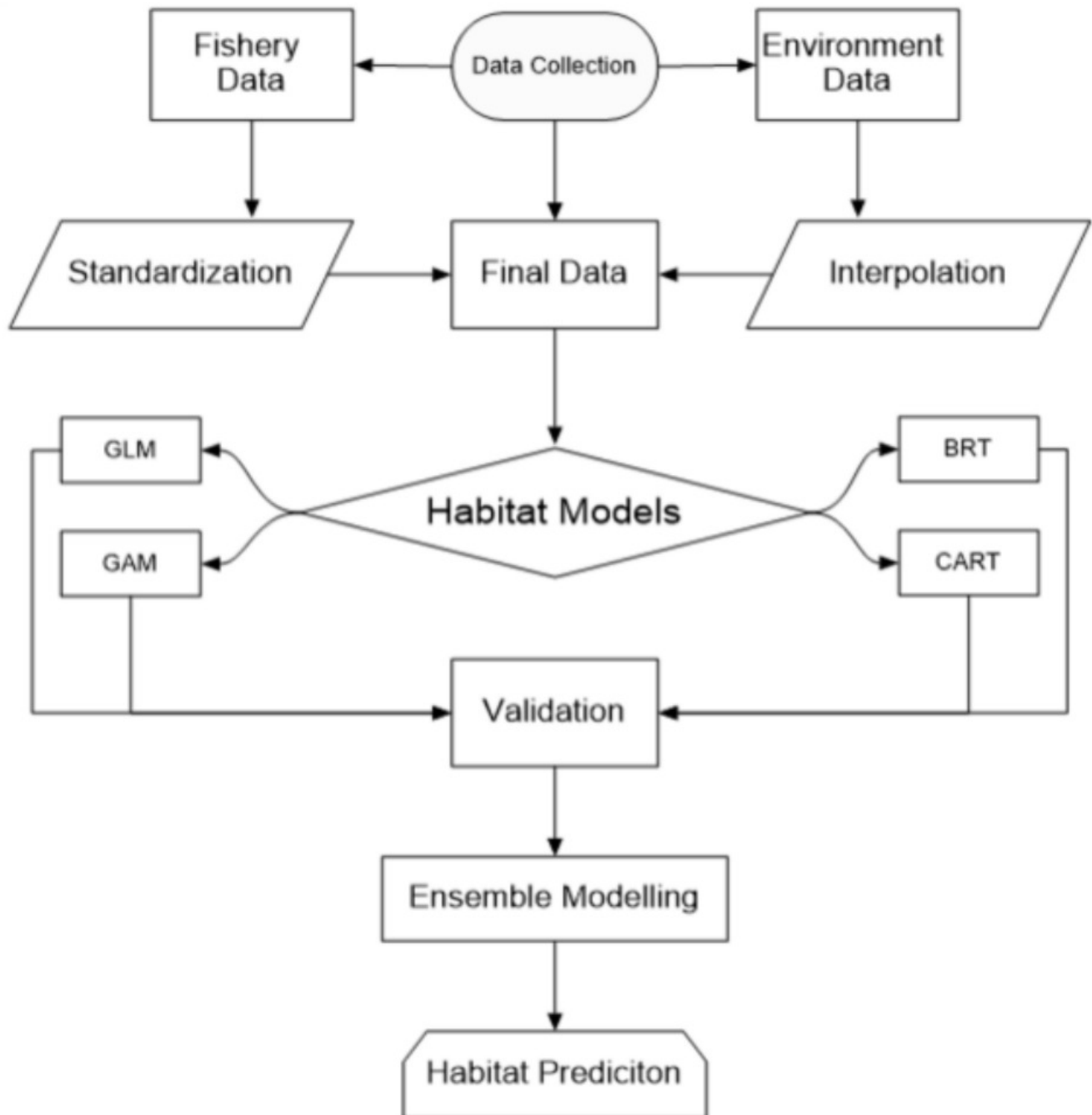


Figure 2

Catches from fishing with different gear

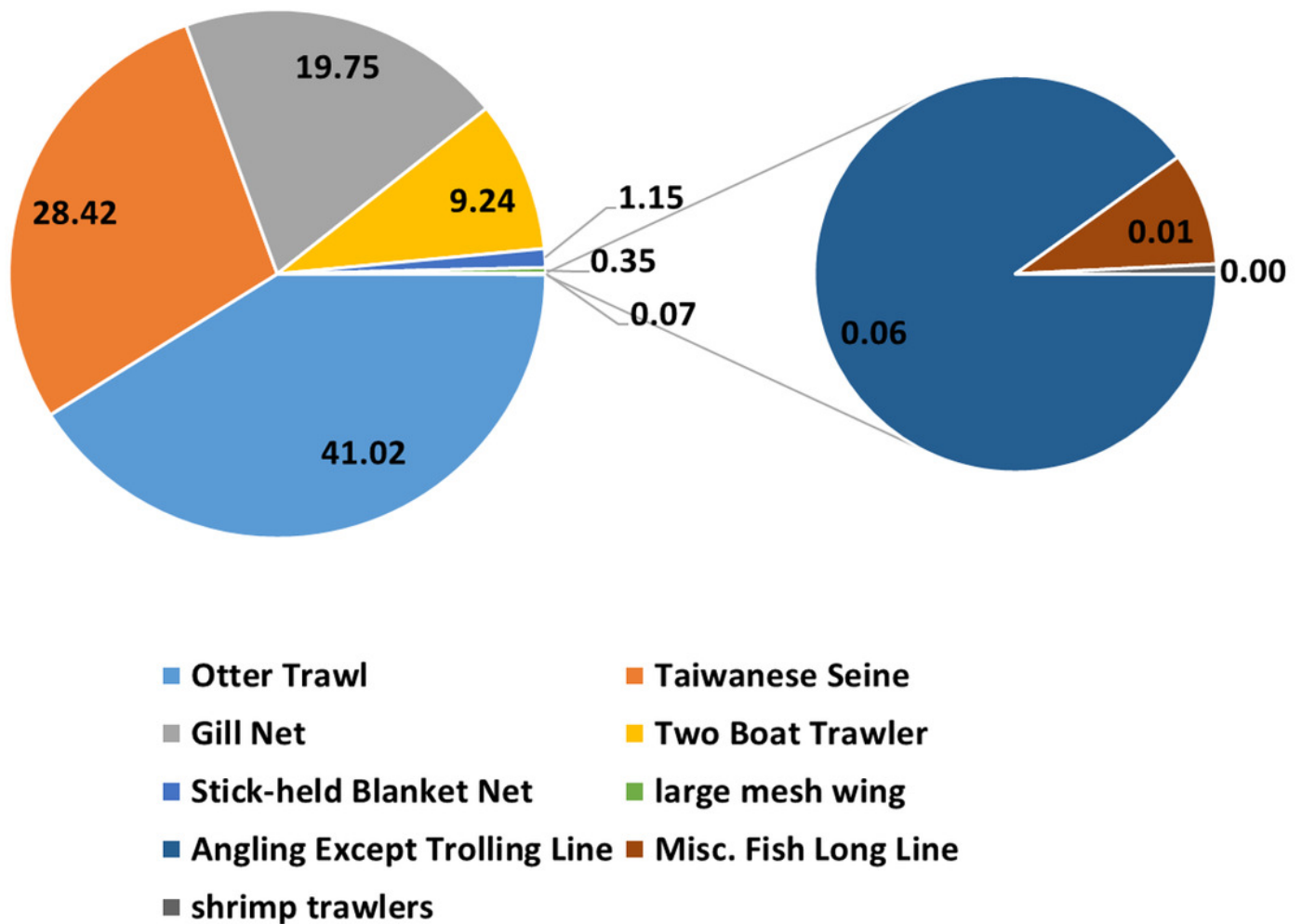
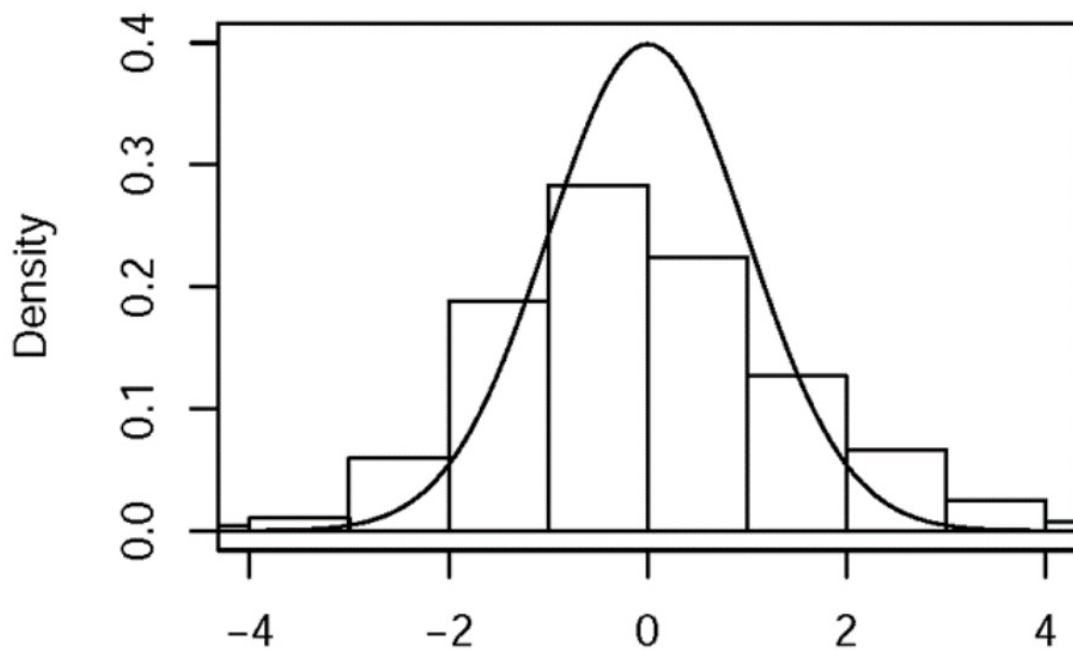


Figure 3

Residual distributions and QQ graphs for the final GLM with predictor variables

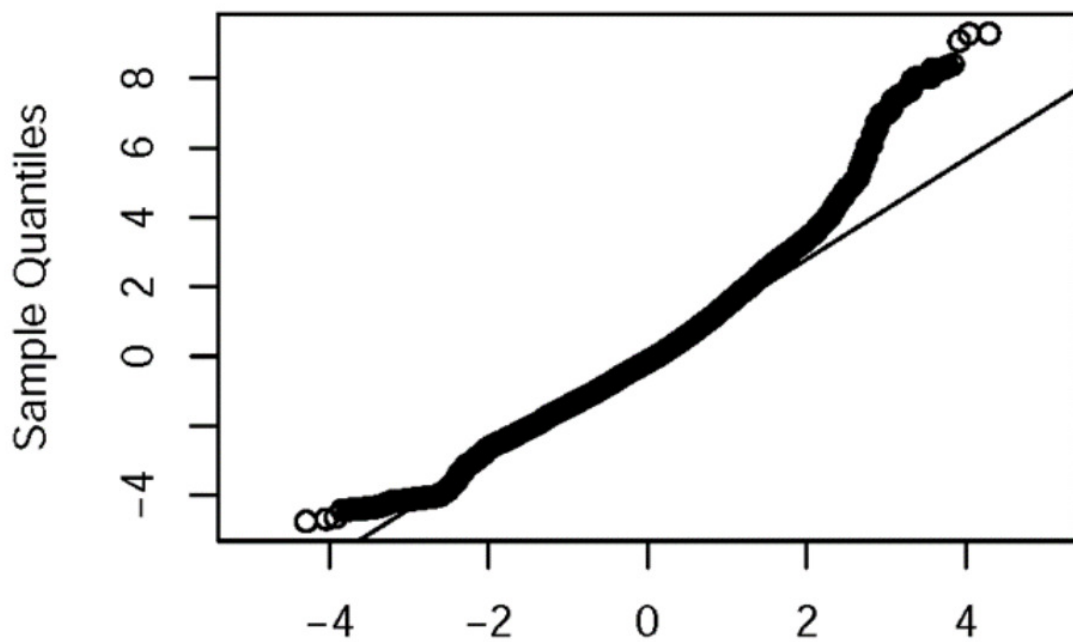
Distribution



(a)

Residuals

QQ Plot



(b)

Theoretical Quantiles

Figure 4

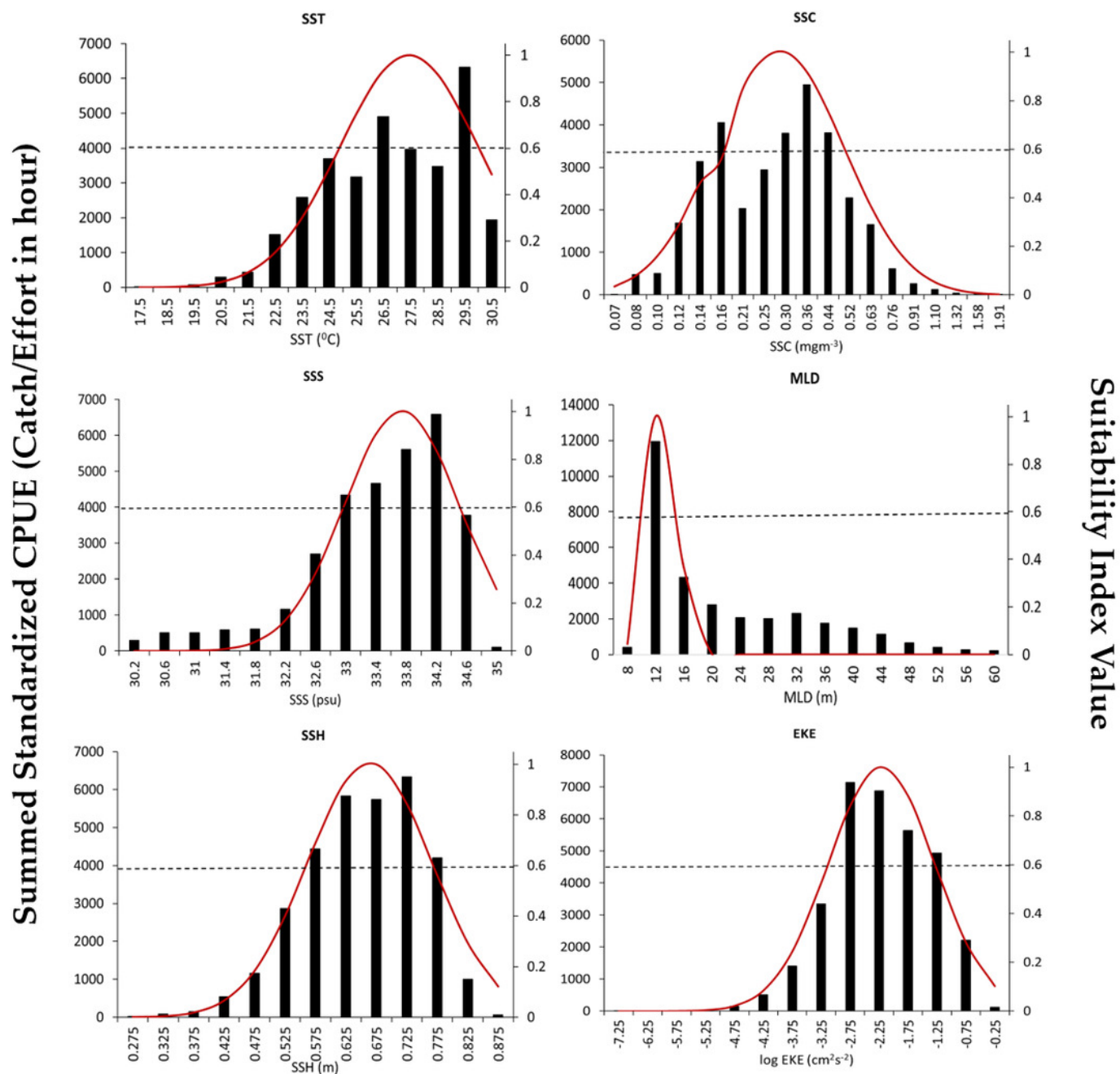
Environmental ranges of *P. niger* with SI values from 2014 to 2019

Figure 5

Residual distributions and QQ plots for diagnostic analysis of the full (a) GAM and (b) GLM, both with predictor variables. Full (c) BRT and (d) CART model performance along with the decision trees of the final model.

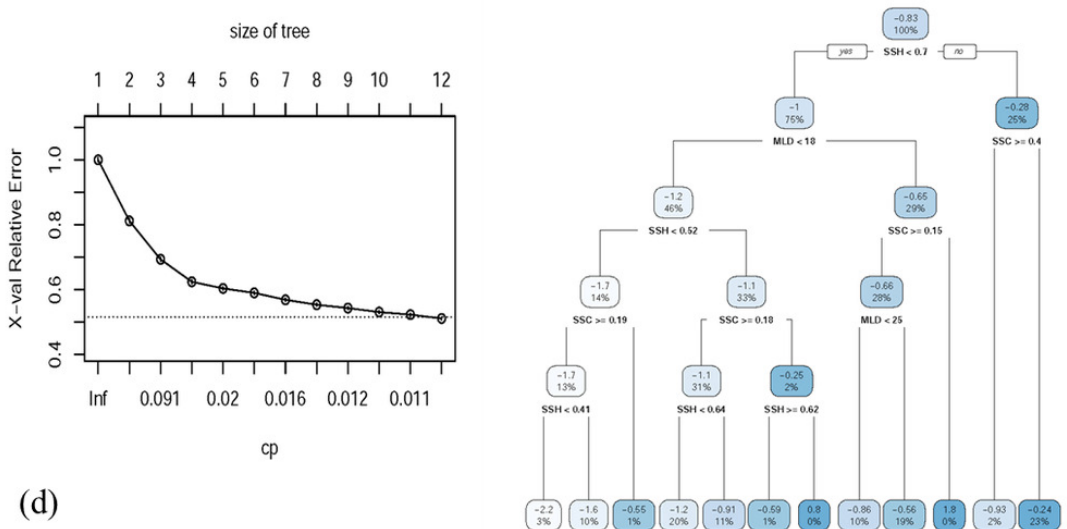
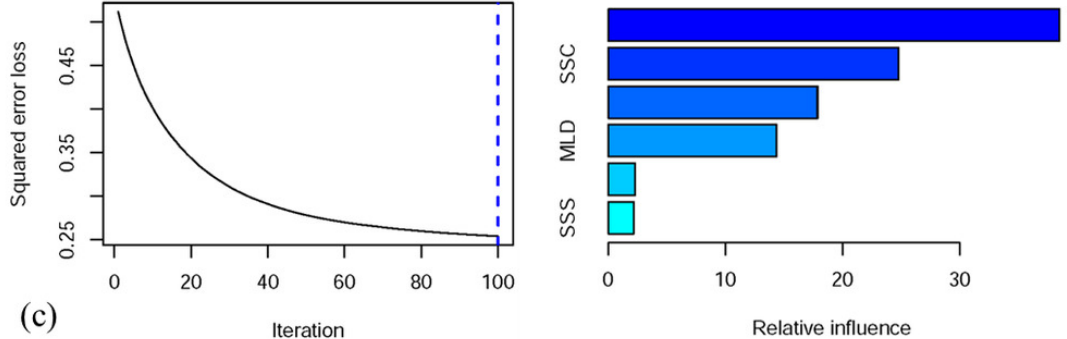
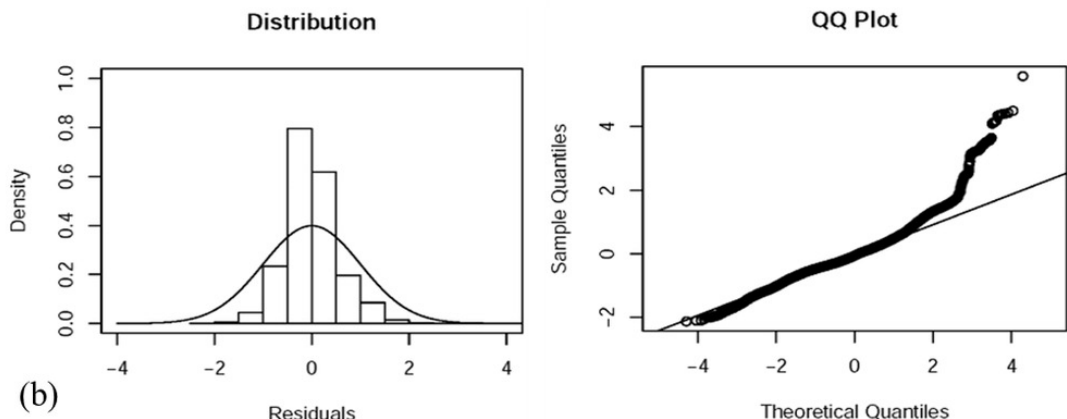
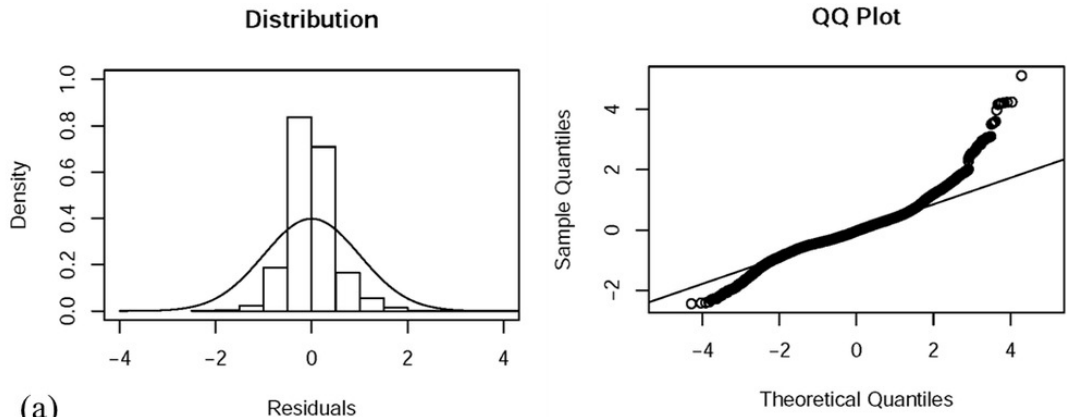


Figure 6

P.CPUE from the ensemble habitat model, along with S.CPUE.

(a) S.CPUE, (b) P.CPUE

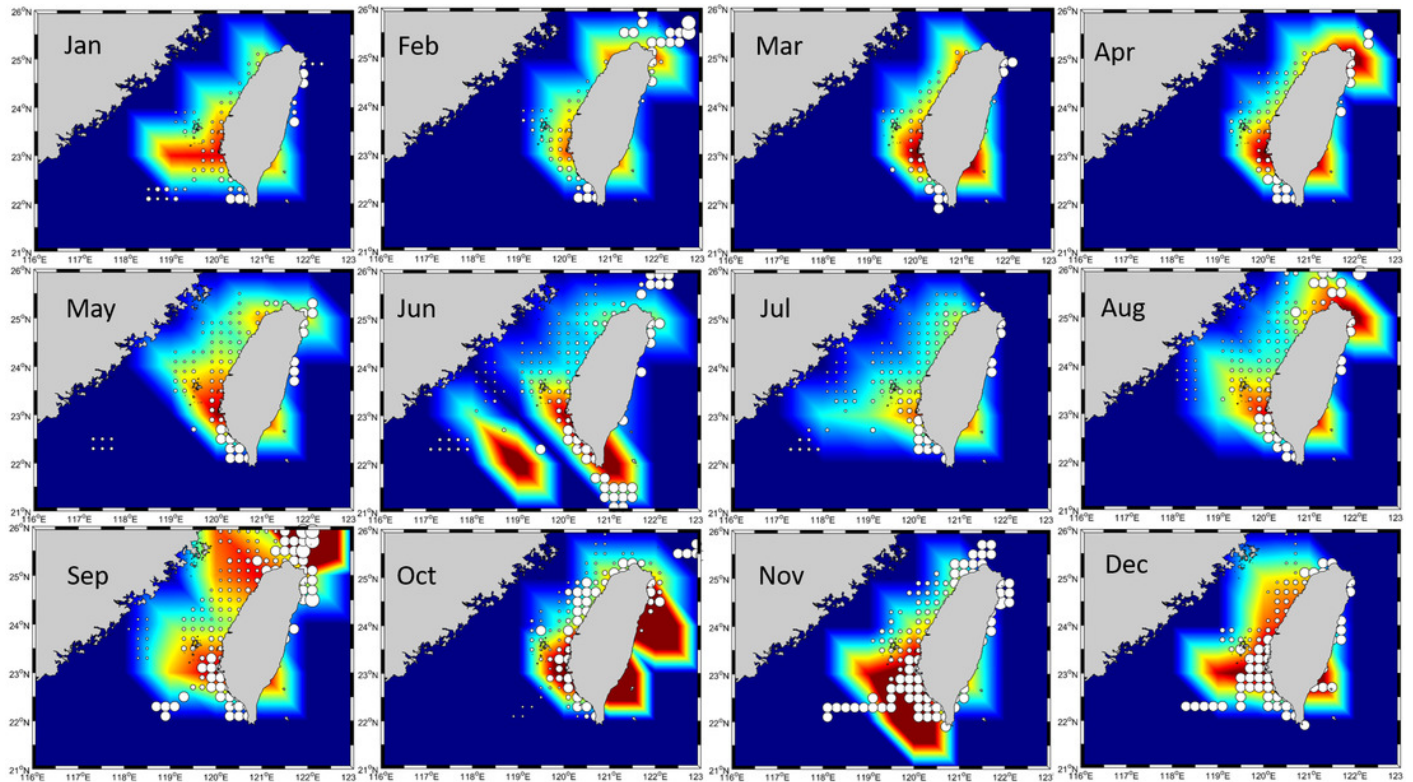


Figure 7

Habitat modeling approach for sustainable development with SDG interactions

